ACS OMEGA

Open Access

http://pubs.acs.org/journal/acsodf

Article

Add-On Device Powered by Parallelized Adsorption Traps for Preconcentrator-GC−MS Measurement of sub-pmol/mol Levels of NF_3

Jeong Sik Lim,* Doohyun Yoon,‖ Taewan Kim,‖ and Jinbok Lee

Cite This: *ACS Omega* 2024, 9, 37225−37230

Read Online

ACCESS | Metrics & More | Article Recommendations

ABSTRACT: In this study, an add-on preconcentration device powered by parallelized pretraps (PPTs) was utilized to measure the sub-pmol/mol levels of NF_3 in N_2. The add-on preconcentrator was coupled to the detachable trap preconcentrator (DTP) with a gas chromatograph−mass spectrometer [*Anal. Chem.* **2019, 91,** 3342−3349]. The breakthrough volume of the parallel configuration was found to be substantially higher than that of the serial configuration with the same amount of adsorbent (HayeSep D). Liquid oxygen (LO_2) cooling (−183 °C) exhibited better preconcentration performance for NF_3 in N_2 compared to NF_3 in air (N_2 + O_2) with liquid nitrogen cooling (−195 °C) and NF_3 in air with LO_2 cooling. The DTP unit was essential to discriminate residual species, such as N_2, O_2, CO_2, and CF_4, of which the preconcentrated portion in the PPT can be excessive, enabling the overwhelm filtering capability of the quadrupole mass spectrometer. The limit of detection of NF_3 in N_2 of the PPT/DTP/gas chromatograph−mass spectrometer was 0.01 ppt, which is significantly better than that determined without using the add-on preconcentration device (0.21 ppt).

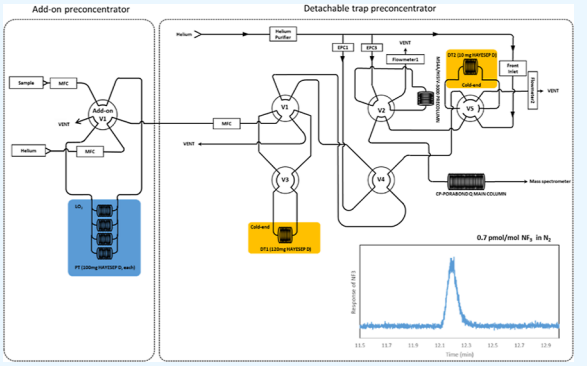

1. INTRODUCTION

Nitrogen trifluoride (NF_3) is a long-lived greenhouse gas (GHG) with an atmospheric lifetime of 500 years.[1] Although its concentration in the atmosphere is only approximately 2 pmol/mol, its global warming potential value at the 100 year scale (GWP_{100}) is 16,100-fold greater than that of carbon dioxide.[1,2] The use of NF_3 has been increasing in the manufacturing of semiconductors, photovoltaic cells, and display devices; consequently, the background concentration of NF_3 in the atmosphere has been increasing by approximately 0.1 pmol/mol per year.[2−4] As a result, NF_3 is now subject to global and regional regulations, making the quantitative assessment of its emissions increasingly critical.[3−5] However, to accurately validate GHG emissions, it is essential to reconcile the discrepancy between the "bottom-up" report of industrial measurements and the "top-down" report of atmospheric measurements.[6,7] To improve the reliability of emission estimates, it is essential to harmonize the measurement values reported by various stakeholders. Achieving this requires the development of suitable and reliable reference materials, along with sensitive and repeatable measurement methods. However, given that the ambient concentration of NF_3 is approximately 2 pmol/mol, preparing and verifying a reference gas mixture (RGM) with acceptable uncertainty present a significant challenge. A previous study of our group reported the limit of detection (LOD) of NF_3 to be 0.2 pmol/mol and measurement precision to be 0.35% (1σ) against an ambient-level sample (2 pmol/mol) using a detachable trap preconcentrator (DTP) with a gas chromatograph−mass spectrometer.[8] However, the DTP/gas chromatograph−mass spectrometer may not provide sufficient measurement capability for the verification of the preparation process of the atmospheric levels of NF_3 in air RGM. One of the primary factors influencing the uncertainty of the RGM in a few pmol/mol is the measurement capability of the target substance presented in the raw gases of matrix components, namely, high-purity N_2 and O_2. For instance, the sensitivity coefficient of SF_6 impurity in N_2 raw gas was 7×10^{11} for the gravimetric preparation of RGM of SF_6 in air.[9] According to ISO 19229:2015, half of the LOD value accounts for the mean value of the nondetected impurity.[10] Therefore, for the verification of an atmospheric-level NF_3 RGM (~2 pmol/mol), the LOD must be improved to achieve an unbiased reference value of the RGM and improved uncertainty. Long-term monitoring data of NF_3 reported by the AGAGE, of

Received: May 17, 2024
Revised: July 22, 2024
Accepted: July 23, 2024
Published: August 21, 2024

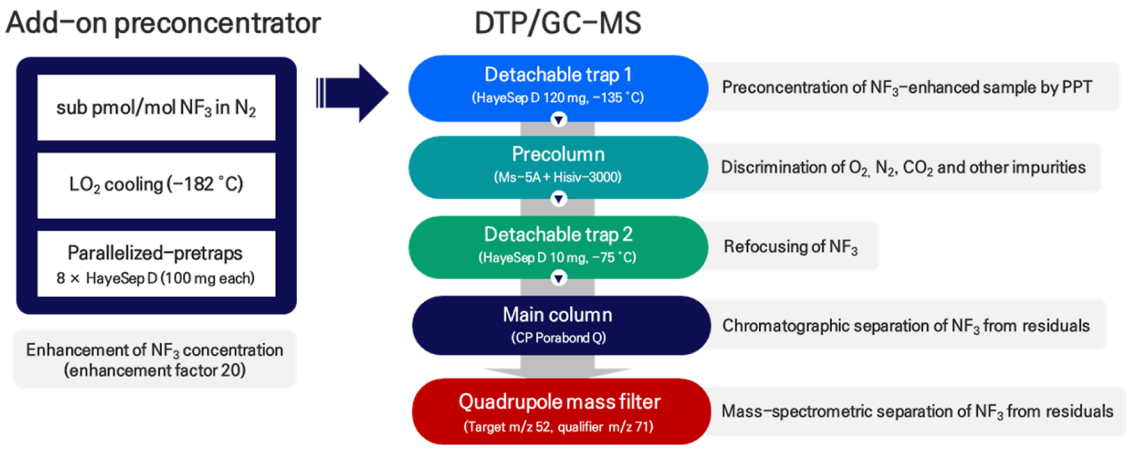

Figure 1. Overview of the instrumental configuration of the add-on preconcentrator powered by eight PPTs and the DTP/gas chromatograph−mass spectrometer. Functionality of each component is given in the gray box.

which the calibration standard was maintained by the Scripps Institute of Oceanography (SIO-12, gravimetric, 2% uncertainty), is the only result publicly available up to date.[11] By the same group, a clear pattern of monthly NF_3 variation has been shown with a measurement precision of 2% (1σ).[5] However, improved uncertainty (combined uncertainties of RGM, calibration, and long-term reproducibility) and harmonized measurement among various observation networks have the potential to help a emission tracking model in greater spatial resolution, allowing for region-specific emission estimates.[12−15] The present study demonstrates an improved analytical capability for determining the LOD of atmospheric-level NF_3 using an add-on preconcentration device, which was powered by parallelized pretraps (PPTs), coupled with a DTP−gas chromatograph−mass spectrometer. The analytical method was optimized by adjusting several factors, including the cooling temperature, number of traps, amount of adsorbent, and feeding flow rate of the sample. Because the LOD is well correlated to the measurement precision around the limit of quantification level,[8] the LOD test can be a representative parameter of the measurement capability for the trace-level NF_3 at sub-pmol/mol concentrations.

2. EXPERIMENTAL SECTION

To enhance the preconcentration volume for the atmospheric level of NF_3, PPTs were added to the DTP/gas chromatograph−mass spectrometer (the gas chromatograph−mass spectrometer was Agilent 7890, 5957C), as published in the previous study of our group.[8] In general, to enhance the detection sensitivity (= MS (mass spectrometric) response/concentration) when using a preconcentrator, the preconcentration volume of the analyte can be increased by decreasing the flow rate of the analyte stream or the preconcentration dwell time. Alternatively, the size of the preconcentration trap, i.e., the amount of adsorbent, can be increased to enlarge the preconcentration volume. In addition, the PPTs must be cooled to enhance the adsorption rate. However, these enhancements are often restricted by the capacity of a cooling instrument. For instance, the DTP/gas chromatograph−mass spectrometer showed that the trap temperature with the PCC Cryotiger PT-14 could not be reduced below −130 °C owing to the limitations of the thermal capacitance of the cold end. Therefore, an extra cooling source such as liquid nitrogen (LN_2, boiling point −195 °C) or liquid oxygen (LO_2, bp −183 °C) is required. In this study, PPTs were added on to the DTP/gas chromatograph−mass spectrometer. HayeSep D 100/120 was placed in a stainless-steel tube (1/8 in.) and blocked with silanized glass wool to hold the adsorbent granules during gas flow (Figure 1). The trap configurations tested in this study are listed in Table 1. The detection sensitivity depends on the loading amount of the adsorbent. The detection sensitivities of single tubes (100 and 1000 mm) and parallelized tubes (4 and 8 mm each) were compared. Before desorption, the PPT was backflushed with high-purity helium. The cooled DTP was removed from the cold dewar and placed in boiling water with a constant carrier gas (He, 99.999%) flowing into the DTP−gas chromatograph−mass spectrometer (Figure 2). The gas chromatograph−mass spectrometer was operated in the selective ion-monitoring mode at a target mass-to-charge ratio (m/z) of 52 and a qualifier m/z of 71. Gravimetrically prepared NF_3 in N_2 gas mixtures was analyzed to the performance of the add-on preconcentrator. NF_3 in N_2 or air gas mixtures was prepared by using high-purity N_2, O_2 and NF_3 gases. Aluminum cylinders (47 L capacity) with electropolished inner surfaces were evacuated to approximately 1×10^{-6} Torr before being used as containers of the NF_3/N_2 and NF_3/air gas mixtures. Further, 0.7 pmol/mol levels of NF_3 in N_2 or air were fed into the PPT by using a well-calibrated mass flow controller (Brooks Instruments). The amount of sample was quantified by multiplying the flow rate by the preconcentration time.

Table 1. Types of Traps for the Add-on Preconcentrator Tested in This Study[a]

	adsorbent	length	adsorbent weight	number of trap
short pretrap	HayeSep D 100/120	100 mm	100 mg	1
long pretrap	HayeSep D 100/120	1000 mm	1000 mg	1
4 parallelized pretrap (4-PPT)	HayeSep D 100/120	100 mm, each	100 mg, each	4
8 parallelized pretrap (8-PPT)	HayeSep D 100/120	100 mm, each	100 mg, each	8

[a]The inner diameter of the tubes was 1/8 in.

https://doi.org/10.1021/acsomega.4c04563
ACS Omega 2024, 9, 37225−37230

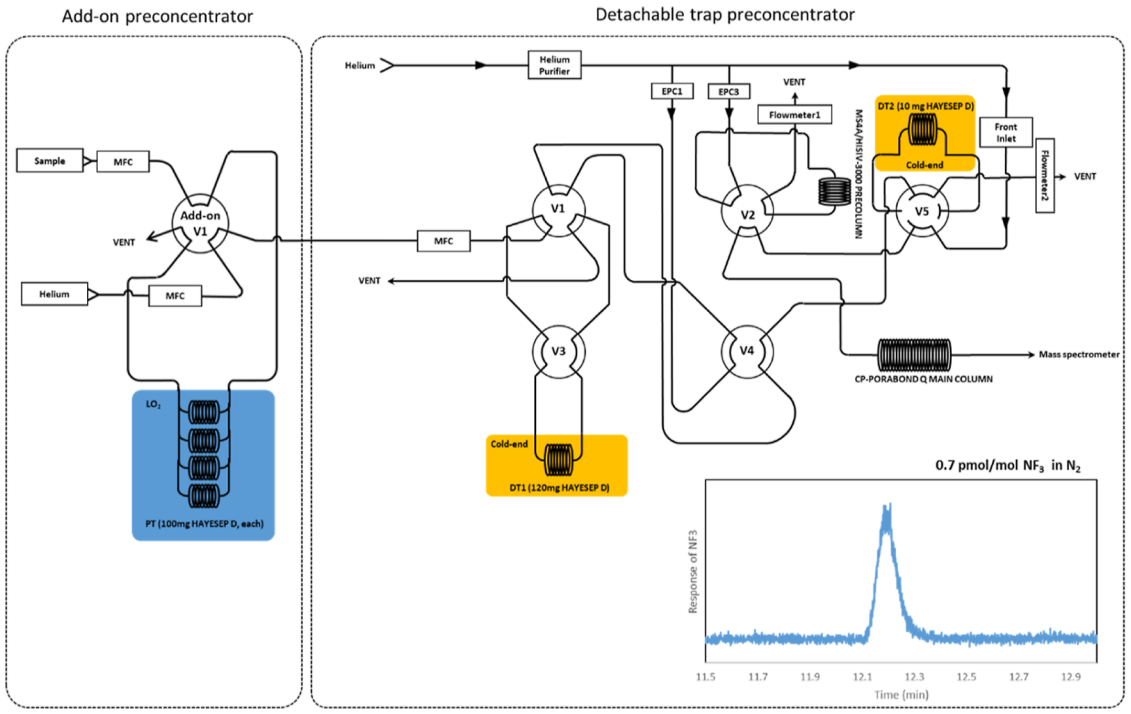

Figure 2. Schematics of the add-on preconcentrator equipped with a parallelized configuration of HayeSep D adsorbent pretraps cooled by LO_2. Preconcentrated NF_3 was directed through the detachable traps to effectively separate potent residuals of the matrix and impurities. The chromatogram (inset) was obtained using 0.7 pmol/mol of NF_3 in N_2. PT denotes the pretrap, DT represents the detachable trap, MFC indicates the mass flow controller, EPC stands for the electric pressure controller, and V denotes the valve.

3. RESULTS AND DISCUSSION

3.1. Cooling Temperature Effect. The detection sensitivity for NF_3 was investigated in various thermodynamical environments (Figure 3). A short pretrap (HayeSep D 100/120, 100 mg) was employed at a flow rate of 1600 mL/min. Adsorptivity of NF_3 (bp −129 °C) with the LN_2 cooling (−195 °C) was expected to surpass that with LO_2 cooling (−183 °C). However, the NF_3 detection sensitivity did not improve in either the N_2 matrix with LN_2 cooling or the O_2 matrix with LO_2 cooling, indicating that N_2 and O_2 predominated at their respective boiling points. Conversely, NF_3 in N_2 at the LO_2 temperature exhibited a significant sensitivity enhancement by increasing sampling amount (= flow rate × sampling time), suggesting a release of free adsorption sites for NF_3. Although fine adjustment of the cooling temperature using such a He cooler above the LO_2 temperature may further optimize the detection sensitivity of NF_3 in air, NF_3 in N_2 at the LO_2 temperature serves as the preset condition for subsequent discussion due to the limitations of our resources.

3.2. Parallelized Trap Configuration. To assess the preconcentration efficiencies of various pretrap configurations (Table 1), the detection sensitivities of NF_3 were measured across different sample amounts (Figure 4). With all analytical parameters held constant except for the pretrap configuration, the slope of the tangential line represents the preconcentration efficiency. The 8-PPT demonstrated the most favorable performance in terms of preconcentration efficiency. Notably, the 8-PPT exhibited a linear response to the sampling amount, namely, the preconcentration time, below a sensitivity threshold of 5000. Although the total amount of adsorbent in 8-PPT (800 mg) was lower than that in the long pretrap (1000 mg), the preconcentration efficiency of the 8-PPT

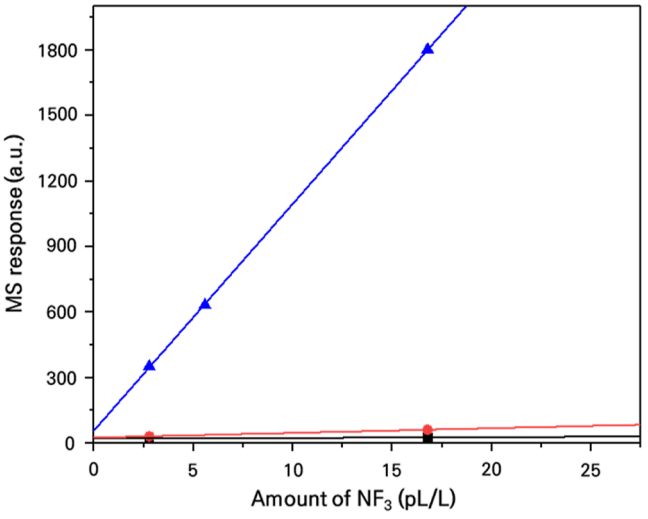

Figure 3. MS response as a function of the amount of NF_3 injected into the add-on preconcentrator. The sensitivity for NF_3 in N_2 increases substantially with respect to the sample amount with LO_2 cooling (blue triangle). Measurements of NF_3 in the air with LO_2 cooling (red circle) and that in N_2 with LN_2 cooling (black rectangular) are not sensitive. A short pretrap (single, HayeSep D 100/120, 100 mg) was used at a flow rate of 1600 mL/min. The amount of NF_3 was estimated by multiplying the sampling flow rate, the preconcentration time, and the concentration of NF_3 (0.7 pmol/mol). The lines are provided as visual guides without any statistical inference.

surpassed that of the long pretrap. Even the 4-PPT (400 mg) demonstrated superior preconcentration efficiency compared to that of the long pretrap (1000 mg). This suggests an increase in the number of active sites for NF_3 in the PPT

https://doi.org/10.1021/acsomega.4c04563
ACS Omega 2024, 9, 37225−37230

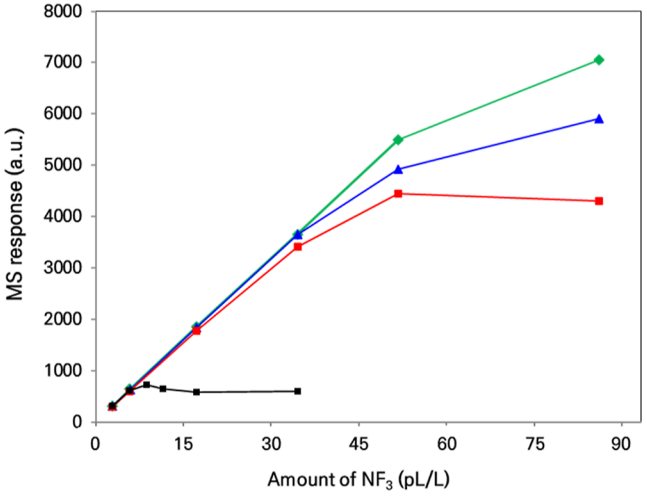

Figure 4. MS response as a function of the amount of NF_3 injected into the add-on preconcentrator, compared across different configurations: 8-PPT (green diamond), 4-PPT (blue triangle), long single pretrap (red rectangle), and short single pretrap (black rectangle). Detailed configurations can be found in Table 1. All measurements were carried out at an identical sample flow rate of 1600 mL/min. The amount of NF_3 was estimated by multiplying the sampling flow rate, the preconcentration time, and the concentration of NF_3 (0.7 pmol/mol). The lines are provided as visual guides without any statistical inference.

configurations. To elucidate this behavior, the Brunauer–Emmett–Teller (BET) isotherm, which is a common adsorption model at low temperatures, provided below can be considered.[16,17]

$$q(p) = q^{sat}\frac{b_s(p)}{(1 - b_l(p))(1 - b_l + b_s(p))} \quad (1)$$

where $q(p)$ is the absolute loading of the adsorbed phase as a function of pressure, q^{sat} is the saturation loading, and b_s and b_l are the equilibrium constants of adsorption on the bare surface and on a layer of previously adsorbed adsorbates, respectively. The BET model extends the Langmuir model by allowing for multilayer formation, where the binding energy of sites in the second layer and beyond is equal to the heat of liquefaction. This model is effective for characterizing various sorbents at low temperatures. It has been reported that the BET isotherm describes the adsorption behaviors of N_2 and CH_4 into the HayeSep D well.[18] HayeSep D demonstrated superior selectivity for CH_4 over N_2 in a stable cold bath at −192 °C. However, NF_3 at 0.7 pmol/mol exhibited lower selectivity to HayeSep D than matrix N_2 at −192 °C (as shown in black in Figure 3). Even at −182 °C, matrix O_2 showed dominant adsorption selectivity to HayeSep D compared to 0.7 pmol/mol of NF_3 (as shown in red in Figure 3). As discussed in the previous section, these phenomena suggest that the adsorption of O_2 and N_2 to HayeSep D significantly increases at their respective boiling points, implying that NF_3 should be mixed with a matrix gas with a boiling point higher than that of the bath coolant. This scenario can be tested by the ideal adsorption solution theory, which can predict multicomponent adsorption isotherms from only the pure-component adsorption isotherms at the same temperature.[17,19] However, the lack of isotherm parameters for NF_3 in HayeSep D results in an incomplete quantitative interpretation of the above scenario. Generally, the component of the binary mixture with the highest saturation loading dominates adsorption at high pressures, potentially displacing the other component (as shown in Figure 3 in ref 17). It should be noted that the optimal isotherm model and equilibrium constants for NF_3 and HayeSep D need to be investigated using a single adsorption bay.[17,19,20]

Qualitatively speaking, trace-level NF_3 mixed with the matrix components had a chance to be adsorbed by free sites in the initial part of the adsorption column. However, free sites in the later part of the pretrap were strongly preferred by the predominant matrix components. Once the adsorption sites are occupied by matrix gas O_2 or N_2 due to high selectivity, it appears that the second layer is filled with the same species, leaving no opportunity for additional adsorption of NF_3. As indicated by the saturated plateau of the sensitivity plot (black in Figure 4), no further adsorption of NF_3 occurred, suggesting the validity of this scenario. The fixed-bed adsorption simulation, a numerical method that takes into account molecular diffusion and mass transfer,[17] can predict the gas uptake of each component of a mixture under flowing conditions. However, the absence of isotherm parameters limits the precise prediction of preconcentration parameters, such as flow rate and preconcentration temperature. Although the lack of isotherm parameters hinders the precise prediction of preconcentration parameters such as the flow rate, amount of absorbent, preconcentration time, and cooling temperature, this limitation was overcome by employing a parallelized configuration of multiple columns with reduced length. As demonstrated in Figure 4, the sensitivity of the 8-PPT (green, with a total of 800 mg of HayeSep D) is even higher than that of a single long trap (red, with a total of 1000 mg of HayeSep D). The number of parallelized traps can be further increased to enhance preconcentration efficiency while maintaining the flow rate at each individual trap.

3.3. Flow Rate Effect. The detection sensitivities of NF_3 at various flow rates (1600, 2000, 2400, and 3200 mL/min) with the 8-PPT were tested to address the dynamic isotherm. For further analysis, the modified Wheeler model (MHM) can be considered (eq 2). The breakthrough volume was defined as an appropriate collection volume for a sample mixture in which the analyte does not pass through the adsorbent beds during preconcentration[21]

$$V_b = \frac{W_e \cdot W_b}{C_0}\left[1 - \frac{1}{k_a \cdot \tau}\ln\left(\frac{C_0}{C_x}\right)\right] \quad (2)$$

where W_e is the kinetic adsorption capacity (adsorbate mass/adsorbent mass), $\tau = {W_b}/{(\rho_b \cdot Q)}$ is the residence time (min), ρ_b is the packed adsorbent density (g/cm^3), Q is the volumetric flow rate (cm^3/min), W_b is the adsorbent mass (g), k_a is the adsorption kinetic constant (min^{-1}), C_0 is the inlet concentration (g/cm^3), and C_x is the outlet concentration (g/cm^3). The term $\frac{W_e \cdot W_b}{C_0}$ represents the total preconcentration volume of the sample at C_0 required to reach thermodynamic equilibrium, V_t. The adsorption efficiency corresponds to the term $1 - \frac{1}{k_v \cdot \tau}\ln\left(\frac{C_0}{C_x}\right)$; therefore, $\frac{1}{k_v \cdot \tau}\ln\left(\frac{C_0}{C_x}\right)$ is the fractional unused bed capacity (FUBC) for the adsorbate. The breakthrough volume can be interpreted as the preconcentration efficiency in the ideal mass transfer of adsorbed analytes from the PPT to the subsequent stage. The slope of the sensitivity curve remained constant until the flow rate reached

https://doi.org/10.1021/acsomega.4c04563
ACS Omega 2024, 9, 37225−37230

2000 mL/min, indicating an increase in the chance of contact (adsorbate−adsorbent contact rate) with the analyte for adsorption on the seed site (Figure 5). However, when

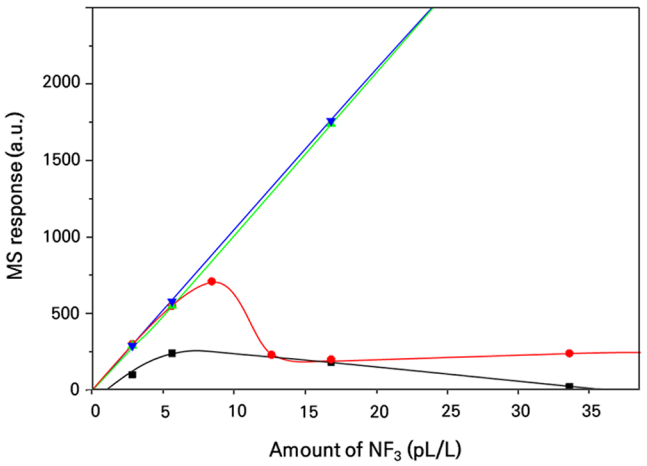

Figure 5. MS response as a function of the amount of NF_3 injected into the add-on preconcentrator, compared across different flow rates: 1600 mL/min (green triangle), 2000 mL/min (blue triangle), 2400 mL/min (red circle), and 3200 mL/min (black rectangle) with 8-PPT. The amount of NF_3 was estimated by multiplying the sampling flow rate, the preconcentration time, and the concentration of NF_3 (0.7 pmol/mol). The lines are provided as visual guides without any statistical inference.

operating at flow rates of >2400 mL/min, a reduction in preconcentration efficiency was noted. This phenomenon could be attributed to the shorter residence time of the analyte in the pretrap. According to the MHM, the breakthrough volume drastically decreases at low residence times, i.e., high flow rates, as demonstrated in our results. However, the residence time only scaled the FUBC. Therefore, the decline in the preconcentration volume can be explained by the conjecture that C_x is higher than C_0, indicating that desorption of the adsorbed NF_3 was activated at high flow rates of the sweep gas N_2.[22] The decline in the preconcentration volume in the short pretrap at 1600 mL/min (black of Figure 4) can be explained by the same origin. Under the same input flow rate, the flow rate at the end point of the short pretrap appeared to be higher in some extent compared to that of the long pretrap due to a weak pressure drop.

4. CONCLUSIONS

This study demonstrated that a parallelized adsorption trap configuration can enhance preconcentration efficiency when coupled with a DTP/gas chromatograph−mass spectrometer. In comparison to the serial configuration, which involves single and elongated columns with similar amounts of adsorbent per unit length, the parallelized configuration preserves active sites for ultratrace level of NF_3 in a flowing condition. Due to the unavailability of adsorption isotherm parameters for NF_3 and N_2 with HayeSep D at −183 °C, precise modeling and trap design were challenging. Despite this constraint, we observed that the 8-PPT configuration (8 × 100 mg) delivered optimal performance at a flow rate of 2000 mL/min for preconcentrating sub-pmol/mol NF_3 in N_2 mixtures. At this temperature and flow rate, the physisorption of N_2 was less effective than under this condition. Therefore, achieving further improvement in NF_3 preconcentration in air using PPTs necessitates temperature adjustment above the LO_2 temperature, which can be achieved with refrigerant-based cooling devices such as a He cooler with a temperature compensating unit. While fine temperature adjustment was not pursued in this study, it presents a complementary approach for NF_3 preconcentration, which could enhance the measurement capability of advanced preconcentration technologies like Medusa-like preconcentrators.[5,8,23−25] Experimental and theoretical determination of adsorption isotherm parameters and model for N_2, O_2, and NF_3 with HayeSep D at temperatures other than LN_2 is imperative to further enhance the preconcentration efficiency of atmospheric NF_3 samples. Nevertheless, the incorporation of PPT add-on devices substantially improved the detection sensitivity of NF_3 by a factor of 20 compared to that obtained using a bare DTP/gas chromatograph−mass spectrometer, with an LOD of NF_3 at 0.2 ppt. This enhancement facilitates high-quality measurement of sub-pmol/mol levels of NF_3 for gravimetric standard preparation and atmospheric NF_3 monitoring. It is noteworthy that DTP- or Medusa-based preconcentrators are essential for discriminating interfering substances, such as CO_2, N_2, O_2, and CF_4, preconcentrated in the PPT. These substances can interfere with the chromatogram of NF_3 due to excessive appearance by substantial ultracold physisorption at LO_2 and LN_2 temperatures.

AUTHOR INFORMATION

Corresponding Author

Jeong Sik Lim − *Precision Measurement, University of Science and Technology (UST), Daejeon 34113, Republic of Korea; Semiconductor and Display Metrology Group, Korea Research Institute of Standards and Science (KRISS), Daejeon 34113, Republic of Korea;* orcid.org/0000-0002-7326-1725; Email: lim.jeongsik@kriss.re.kr

Authors

Doohyun Yoon − *Precision Measurement, University of Science and Technology (UST), Daejeon 34113, Republic of Korea; Semiconductor and Display Metrology Group, Korea Research Institute of Standards and Science (KRISS), Daejeon 34113, Republic of Korea*

Taewan Kim − *Precision Measurement, University of Science and Technology (UST), Daejeon 34113, Republic of Korea; Semiconductor and Display Metrology Group, Korea Research Institute of Standards and Science (KRISS), Daejeon 34113, Republic of Korea;* orcid.org/0000-0003-0491-4216

Jinbok Lee − *Gas Metrology Group, Korea Research Institute of Standards and Science (KRISS), Daejeon 34113, Republic of Korea*

Complete contact information is available at: https://pubs.acs.org/10.1021/acsomega.4c04563

Author Contributions

‖D.Y. and T.K. equally contributed to this work.

Notes

The authors declare no competing financial interest.

ACKNOWLEDGMENTS

The authors thank for fruitful discussion by Dr. Jeongsoon Lee and financial support by Dr. Dohyun Kwon. This work was funded by the Korea Meteorological Administration (KMA) under the project of development of continuous measurement

https://doi.org/10.1021/acsomega.4c04563
ACS Omega 2024, 9, 37225−37230

of halogenated greenhouse gases at the background atmospheric concentration level (KMI2022-01410), the Ministry of Trade, Industry and Energy (MOTIE) under the project of development of monitoring and analysis technologies for greenhouse gases in the semiconductor manufacturing etching process (RS-2023-00265582), and the Korea Research Institute of Standards and Science (KRISS) under the basic R&D project of establishing measurement standards for climate monitoring based on molecular spectroscopy (grant no. 24011107).

REFERENCES

(1) Chen, D.; Rojas, M.; Samset, B. H.; Cobb, K.; Diongue-Niang, A.; Edwards, P.; Emori, S.; Faria, S. H.; Hawkins, E.; Hope, P.; Huybrechts, P.; Meinshausen, M.; Mustafa, S. K. E. A. R.; Plattner, G.-K.; Treguier, A. M.; Lai, H.-W.; Villaseñor, T.; Barimalala, R.; Carmona, R.; Cox, P. M.; Cramer, W.; Doblas-Reyes, F. J.; Dolman, H.; Dosio, A.; Eyring, V.; Flato, G. M.; Forster, P.; Frame, D.; Frieler, K.; Fuglestvedt, J. S.; Fyfe, J. C.; Garschagen, M.; Gergis, J.; Gillett, N. P.; Grose, M.; Guilyardi, E.; Guivarch, C.; Hassol, S.; Hausfather, Z.; Hersbach, H.; Hewitt, H. T.; Howden, M.; Huggel, C.; Hurlbert, M.; Jones, C.; Jones, R. G.; Kaufman, D. S.; Kopp, R. E.; Leiserowitz, A.; Lempert, R. J.; Lewis, J.; Liao, H.; Lovenduski, N.; Lund, M. T.; Mach, K.; Maraun, D.; Marotzke, J.; Minx, J.; Nicholls, Z. R. J.; O'Neill, B. C.; Ogaz, M. G.; Otto, F.; Parker, W.; Parmesan, C.; Pearce, W.; Pedace, R.; Reisinger, A.; Renwick, J.; Riahi, K.; Ritchie, P.; Rogelj, J.; Sapiains, R.; Satoh, Y.; Seneviratne, S. I.; Shepherd, T. G.; Sillmann, J.; Silva, L.; Slangen, A. B. A.; Sörensson, A. A.; Steinle, P.; Stocker, T. F.; Stockhause, M.; Stone, D.; Swann, A.; Szopa, S.; Takayabu, I.; Tebaldi, C.; Terray, L.; Thorne, P. W.; Trewin, B.; Trigo, I.; van Aalst, M. K.; van den Hurk, B.; van Vuuren, D.; Vautard, R.; Vera, C.; Viner, D.; von Engeln, A.; von Schuckmann, K.; Zhang, X.; Chuersuwan, N.; Hegerl, G.; Yasunari, T.; Lai, H.-W.; Villaseñor, T. *IPCC Sixth Assessment Report (AR6) Working Group 1: the Physical Science Basis*; University Press: UK, 2021; Vol. 7.http://www.ipcc.ch/report/ar6/wg1/downloads.

(2) Trisna, B. A.; Park, S. N.; Park, I.; Lee, J.; Lim, J. S. Measurement Report: Radiative Efficiencies of $(CF_3)_2CFCN$, CF_3OCFCF_2, and $CF_3OCF_2CF_3$. *Atmos. Chem. Phys.* **2023**, *23* (7), 4489−4500.

(3) Weiss, R. F.; Mühle, J.; Salameh, P. K.; Harth, C. M. Nitrogen Trifluoride in the Global Atmosphere. *Geophys. Res. Lett.* **2008**, *35* (20), 1−3.

(4) Arnold, T.; Harth, C. M.; Mühle, J.; Manning, A. J.; Sala-meh, P. K.; Kim, J.; Ivy, D. J.; Steele, L. P.; Petrenko, V. V.; Severinghaus, J. P.; Baggenstos, D.; Weiss, R. F. Nitrogen Trifluoride Global Emissions Estimated from Updated Atmospheric Measurements. *Proc. Natl. Acad. Sci. U.S.A.* **2013**, *110* (6), 2029−2034.

(5) Arnold, T.; Mühle, J.; Salameh, P. K.; Harth, C. M.; Ivy, D. J.; Weiss, R. F. Automated Measurement of Nitrogen Trifluoride in Ambient Air. *Anal. Chem.* **2012**, *84* (11), 4798−4804.

(6) Weiss, R. F.; Prinn, R. G. Quantifying Greenhouse-gas Emissions from Atmospheric Measurements: A Critical Reality Check for Climate Legislation. *Philos. Trans. R. Soc., A* **2011**, *369* (1943), 1925−1942.

(7) Arnold, T.; Manning, A. J.; Kim, J.; Li, S.; Webster, H.; Thomson, D.; Mühle, J.; Weiss, R. F.; Park, S.; O'Doherty, S. Inverse Modelling of CF_4 and NF_3 Emissions in East Asia. *Atmos. Chem. Phys.* **2018**, *18* (18), 13305−13320.

(8) Yoon, D.; Lee, J.; Lim, J. S. Detachable Trap Preconcentrator with a Gas Chromatograph−Mass Spectrometer for the Analysis of Trace Halogenated Greenhouse Gases. *Anal. Chem.* **2019**, *91* (5), 3342−3349.

(9) Lim, J. S.; Lee, J.; Moon, D.; Kim, J. S.; Lee, J.; Hall, B. D. Gravimetric Standard Gas Mixtures for Global Monitoring of Atmospheric SF_6. *Anal. Chem.* **2017**, *89* (22), 12068−12075.

(10) ISO. *Gas Analysis-Purity Analysis and the Treatment of Purity Data*. ISO 19229:2019.

(11) Prinn, R. G.; Weiss, R. F.; Arduini, J.; Arnold, T.; Fraser, P. J.; Ganesan, A. L.; Gasore, J.; Harth, C. M.; Hermansen, O.; Kim, J.; Krummel, P. B.; Li, S.; Loh, Z. M.; Lunder, C. R.; Maione, M.; Manning, A. J.; Miller, B. R.; Mitrevski, B.; Mühle, J.; O'Doherty, S.; Park, S.; Reimann, S.; Rigby, M.; Salameh, P. K.; Schmidt, R.; Simmonds, P. G.; Steele, L. P.; Vollmer, M. K.; Wang, R. H.; Young, D. *The ALE/GAGE/AGAGE Data Base*. http://agage.mit.edu/data.

(12) Kim, J.; Li, S.; Kim, K. R.; Stohl, A.; Mühle, J.; Kim, S. K.; Park, M. K.; Kang, D. J.; Lee, G.; Harth, C. M.; Salameh, P. K.; Weiss, R. F. Regional Atmospheric Emissions Determined from Measurements at Jeju Island, Korea: Halogenated Compounds from China. *Geophys. Res. Lett.* **2010**, *37*, L12801.

(13) Stohl, A.; Kim, J.; Li, S.; O'Doherty, S.; Mühle, J.; Salameh, P. K.; Saito, T.; Vollmer, M. K.; Wan, D.; Weiss, R. F.; Yao, B.; Yokouchi, Y.; Zhou, L. X. Hydrochlorofluorocarbon and Hydrofluorocarbon Emissions in East Asia Determined by Inverse Modeling. *Atmos. Chem. Phys.* **2010**, *10* (8), 3545−3560.

(14) Li, S.; Kim, J.; Kim, K.-R.; Mühle, J.; Kim, S.-K.; Park, M.-K.; Stohl, A.; Kang, D.-J.; Arnold, T.; Harth, C. M.; Salameh, P. K.; Weiss, R. F. Emissions of Halogenated Compounds in East Asia Determined from Measurements at Jeju Island, Korea. *Environ. Sci. Technol.* **2011**, *45* (13), 5668−5675.

(15) Saito, T.; Yokouchi, Y.; Stohl, A.; Taguchi, S.; Mukai, H. Large Emissions of Perfluorocarbons in East Asia Deduced from Continuous Atmospheric Measurements. *Environ. Sci. Technol.* **2010**, *44* (11), 4089−4095.

(16) Camara, M.; Breuil, P.; Briand, D.; Viricelle, J.-P.; Pijolat, C.; de Rooij, N. F. Preconcentration Modeling for the Optimization of a Micro Gas Preconcentrator Applied to Environmental Monitoring. *Anal. Chem.* **2015**, *87* (8), 4455−4463.

(17) Sharma, S.; Balestra, S. R. G.; Baur, R.; Agarwal, U.; Zuidema, E.; Rigutto, M. S.; Calero, S.; Vlugt, T. J. H.; Dubbeldam, D. R. U. P. T. U. R. A. RUPTURA: simulation code for breakthrough, ideal adsorption solution theory computations, and fitting of isotherm models. *Mol. Simul.* **2023**, *49* (9), 893−953.

(18) Eyer, S.; Stadie, N.; Borgschulte, A.; Emmenegger, L.; Mohn, J. Methane Preconcentration by Adsorption: a Methodology for Materials and Conditions Selection. *Adsorption* **2014**, *20*, 657−666.

(19) Simon, C. M.; Smit, B.; Haranczyk, M. pyI. A. S. T. pyIAST: Ideal adsorbed solution theory (IAST) Python package. *Comput. Phys. Commun.* **2016**, *200*, 364−380.

(20) Mason, J. A.; McDonald, T. M.; Bae, T.-H.; Bachman, J. E.; Sumida, K.; Dutton, J. J.; Kaye, S. S.; Long, J. R. Application of a High-Throughput Analyzer in Evaluating Solid Adsorbents for Post-Combustion Carbon Capture via Multicomponent Adsorption of CO_2, N_2, and H_2O. *J. Am. Chem. Soc.* **2015**, *137*, 4787−4803.

(21) Lu, C.-J.; Zellers, E. T. A Dual-Adsorbent Preconcentrator for a Portable Indoor-VOC Microsensor System. *Anal. Chem.* **2001**, *73* (14), 3449−3457.

(22) Sukaew, T.; Zellers, E. T. Evaluating the Dynamic Retention Capacities of Microfabricated Vapor Preconcentrators as a Function of Flow Rate. *Sens. Actuators, B* **2013**, *183* (5), 163−171.

(23) Rennick, C.; Arnold, T.; Safi, E.; Drinkwater, A.; Dylag, C.; Webber, E. M.; Hill-Pearce, R.; Worton, D. R.; Bausi, F.; Lowry, D. Boreas: A Sample Preparation-Coupled Laser Spectrometer System for Simultaneous High-Precision In Situ Analysis of $\delta^{13}C$ and $\delta^{2}H$ from Ambient Air Methane. *Anal. Chem.* **2021**, *93* (29), 10141−10151.

(24) Prokhorov, I.; Mohn, J. CleanEx: A Versatile Automated Methane Preconcentration Device for High-Precision Analysis of $^{13}CH_4$, $^{12}CH_3D$, and $^{13}CH_3D$. *Anal. Chem.* **2022**, *94* (28), 9981−9986.

(25) Obersteiner, F.; Bönisch, H.; Keber, T.; O'Doherty, S.; Engel, A. A Versatile, Refrigerant- and Cryogen-free Cryofocusing−thermodesorption Unit for Preconcentration of Traces Gases in air. *Atmos. Meas. Tech.* **2016**, *9*, 5265−5279.

https://doi.org/10.1021/acsomega.4c04563
ACS Omega 2024, 9, 37225−37230